

The Effects of Heavy Charged Particle Irradiation of MOSFET Devices

William Eichinger, Patrick O'Reilly, and Christopher Lehner
Department of Physics, United States Military Academy
West Point, New York 10996

Ionizing cosmic particle radiation poses a serious threat to electronic devices (such as metal-oxide semiconductor, field effect transistors - MOSFETs) that are used in outer space. The physical process in which a bombarding ion creates electron-hole pairs in the SiO₂ layer of a MOSFET, the subsequent collection of charge at the SiO₂-substrate interface and its effect on the operating characteristics of the transistor is modeled with two second order, coupled differential equations. The coupled equations are solved using the finite difference technique known as the Alternating Direction Implicit Method, ADI. Preliminary verification of the computer code was performed using a low energy proton accelerator. The measured change in MOSFET operating characteristics compared favorably with the predicted results. The results show that the damage due to ionizing particles is greatly dependent on the energy of the bombarding particle, its angle of incidence, and the magnitude of the bias applied to the MOSFET.

Introduction.

As our technological exploitation of space progresses, so does our dependence on the reliable operation of electronic devices in the harsh environment of outer space. Cosmic particles (consisting of 85% protons and 14% alpha particles)¹ are a primary threat to the reliable functioning of commonly used electronic devices such as metal-oxide semiconductor, field effect transistors (MOSFETs). MOSFETs are often used because they are easy to fabricate, are relatively impervious to radiation, and have a low noise background, enabling the amplification of extremely weak signals. Payload, weight and speed constraints require that these electronics devices be miniaturized. Unfortunately, as the device parameters decrease, their vulnerability to the ionizing radiation of a single particle (termed a single event upset, SEU) increases, as well as the long term effects of low levels of ionizing radiation. If the effects of ionizing radiation could be understood, then electronic devices could be designed to maximize their survivability in space. The purpose of this paper is to present the results of a computer code which models the effects of ionizing radiation due to heavy ions in MOSFET devices and preliminary results which verify the code predictions.

Operation of MOSFET Devices.

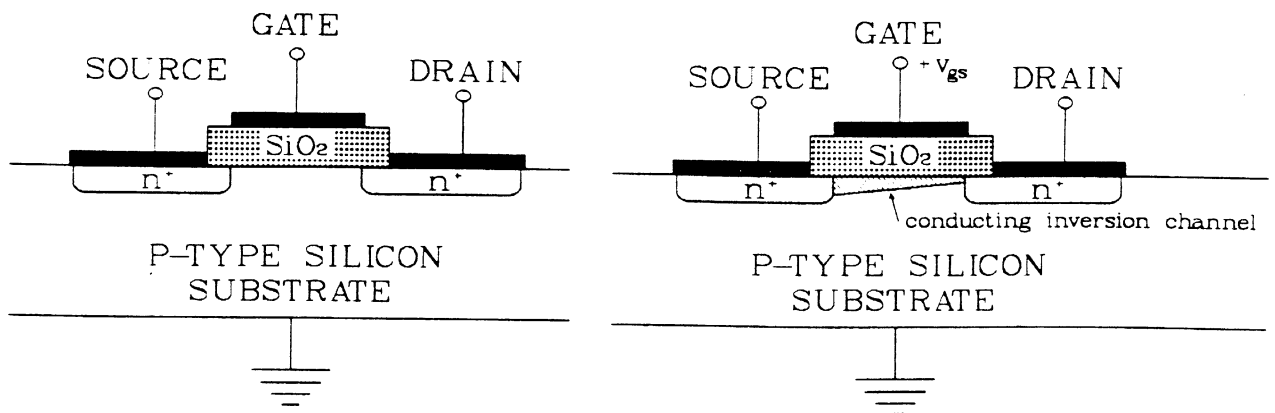


Figure 1a. No Gate Voltage Figure 1b. Positive Gate Voltage
N-Channel Enhancement MOSFET

The electronic device modeled is an enhancement MOSFET (Figure 1a). In the case of an n-channel device, an SiO₂ layer is used to insulate the gate from the p-doped silicon substrate. Although there is not an intrinsic conduction path between the drain and the source, a conducting channel is formed when a positive electric potential (V_{gs}) is placed between the gate and the substrate. This is due to the attraction of electrons to the top of the substrate layer (see figure 1b). These electrons act as the majority carriers in a current (I_d) between the source and the drain which is related to the minimum (or threshold) potential (V_t) required to form the n-channel by:

$$I_d = k(V_{gs} - V_t)^2 \quad (1)$$

where $V_{gs} > V_t$ and k is a device dependent constant. Figure 2 shows the device characteristics for a typical n-channel enhancement MOSFET. P-channel devices may also be constructed which operate in a similar manner².

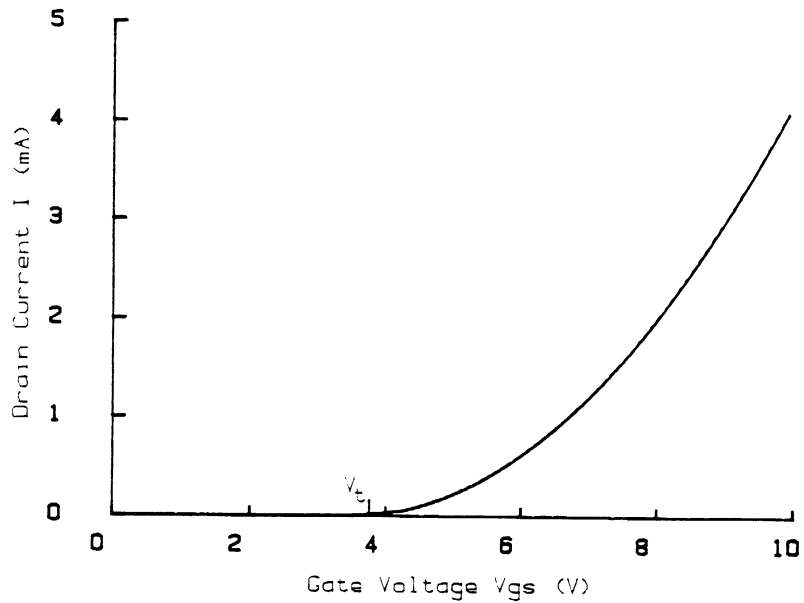


Figure 2. Typical I-V Curve For An N-Channel Enhancement MOSFET.

Damage Mechanisms of Ionizing Radiation In MOSFET Devices.

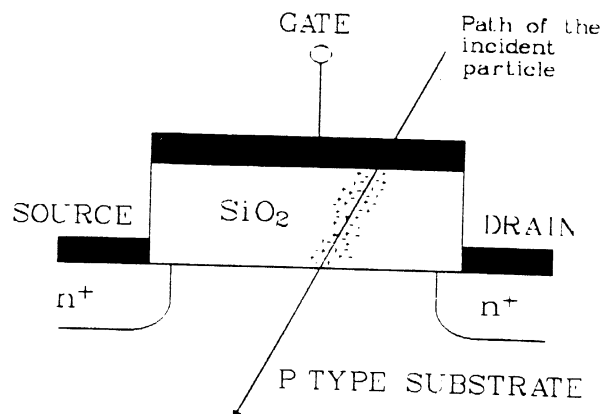


Figure 3. Electron-Hole Generation By Ion Bombardment

When a heavy ion strikes a MOSFET, lattice atoms are ionized as the ion travels through the materials leaving a column of electron-hole pairs as shown in figure 3. In the SiO_2 layer, the electrons are quickly swept away through the gate when V_{gs} is positive. Many of these electrons recombine with the holes as they move toward the gate. The holes which have not recombined will

move to the bottom of the SiO₂ layer, forming a semipermanent concentration of positive charge trapped along the substrate-SiO₂ interface. Consequently, this positive charge will attract electrons in the substrate to the SiO₂-substrate interface decreasing the amount of potential that must be applied to form the n-channel. Thus V_t is reduced by

$$\Delta V_t = - \frac{Q_0 f}{C_{ox}} \quad (2)$$

where Q₀ is the total amount of positive charge deposited in the SiO₂ by the incident particle, f is the fraction of the total charge which does not recombine, and C_{ox} is the SiO₂ capacitance. Sufficient irradiation can cause the required threshold voltage to go to zero, thus permanently forming the n-channel (the transistor will remain on).

Mathematical Model of the Effects of Ionizing Radiation.

The result of a heavy ion's traverse through a layer of SiO₂ was modeled as a concentrated column of electron-hole pairs (figure 4a). The initial volume density of the electron-hole pairs decreases radially from the center of the incident ion's path as represented by:

$$n(r) = \frac{N_0 e^{-r^2/b^2}}{\pi b^2} \quad (3)$$

where n(r) is the volume density of electron-hole pairs, N₀ is the linear density of electron-hole pairs, b is the radius of the column and r is the radial distance from the center of the column.

The density of the holes in the SiO₂ is dependent upon the rate of recombination, the rate of diffusion, and the rate of drift of the holes and electrons due to an applied electric field. This dependence is mathematically expressed by the following coupled set of equations:

$$\frac{\partial n_+(r,t)}{\partial t} = D_+ \nabla^2 n_+(r,t) + \mu_+ E_x \frac{\partial n_+(r,t)}{\partial x} - \alpha n_+(r,t) n_-(r,t) \quad (4)$$

$$\frac{\partial n_-(r,t)}{\partial t} = D_- \nabla^2 n_-(r,t) - \mu_- E_x \frac{\partial n_-(r,t)}{\partial x} - \alpha n_+(r,t) n_-(r,t) \quad (5)$$

where D_± is the diffusion coefficient, μ_± is the mobility of the electrons or holes as appropriate, E_x is the component of the electric field perpendicular to the column, α is the recombination coefficient and n₊ and n₋ are the hole and electron volume densities respectively. These equations were first proposed by George Jaffee in 1913³. The solution to these equations will yield the fraction of the original number of holes which escape recombination and begin to migrate towards the SiO₂ - substrate interface. The first term represents the diffusion of holes in the oxide due to the radial density gradient of the electron-hole pairs. The middle term represents the drift of the holes due to the applied electric field. Since the mobility of the holes is much less than the mobility of the electrons, the holes are essentially stationary for times much longer than the time required for the collection of electrons at the gate (10⁻¹³ seconds). The last term of the equations represents the loss of electrons and holes due to recombination.

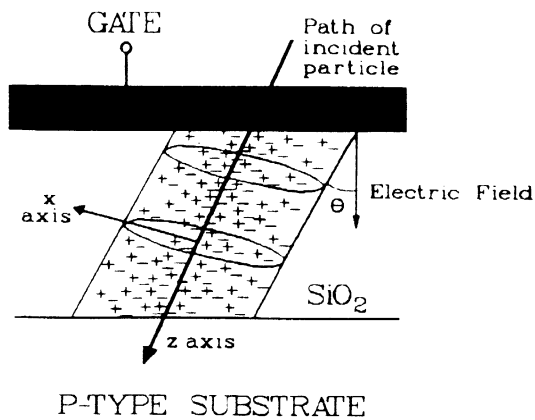


Figure 4a. At Time Equal 0

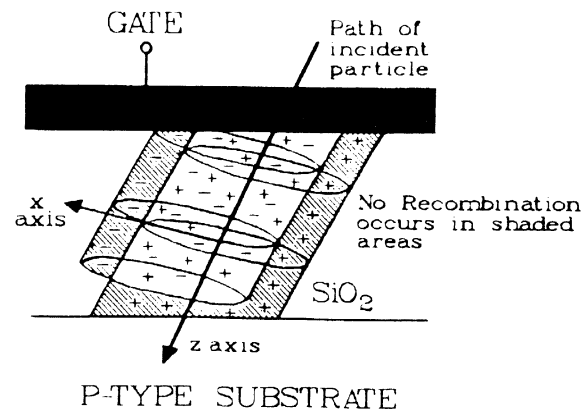


Figure 4b. At Later Times

Figure 4. Charge Movement With Time

Unfortunately, equations 4 and 5 are coupled differential equations which can not be solved analytically using traditional methods of analysis. Thus Jaffee only solved for approximate solutions by ignoring the recombination term and then later attempting to reintroduce its effects. However, with the advent of numerical methods executed by computers, the accurate solution of these equations and the prediction of the effects of ionizing radiation on the MOSFET devices is now possible.

The Computer Model.

The model we have used assumes that two concentric cylinders are formed by the passage of the ion through the SiO_2 layer (see figure 4a). One of the cylinders represents the electron distribution, the other the distribution of holes. The axis of the two concentric cylinders is taken to be the z axis. The angle between the z axis and the normal to the SiO_2 -substrate surface is θ . The electron/hole volume density function is assumed to be gaussian in the x-y plane and symmetric about the z axis and given by equation 3⁴. The linear energy deposition (and thus the electron-hole linear density) of the ion is assumed to be constant over the axial length of the cylinder. This assumption enables the use of a two dimensional solution of the Jaffee Equation since the electrons will not diffuse along the length of the cylinder. The only motion in the axial direction is due to the electric field which will be considered later. The x axis is orthogonal to the cylinder axis and chosen such that the electric field can be expressed completely by its components in the x and z directions.

Each column is conceptually divided into planes which are perpendicular to the column axis. Each plane is subdivided into elements of equal area based upon the choice of Δx and Δy . The electron and hole distribution is evaluated for each element in each time step. These calculated distributions are representative of distributions at any similar point along the z axis. The movement of the cylinders is due to diffusion and the applied electric field. Recombination occurs only where the cylinder of electrons overlaps the cylinder of holes. Movement in the x direction as a result of the x component of the electric field moves the cylinders apart and limits the amount of recombination

that may take place (see figure 4b). Movement in the z direction is due solely to the z component of the electric field. The electrons remaining in those portions of the cylinder which no longer overlap the cylinder of containing holes escape recombination and will be collected at the gate. The number of electrons collected at the gate is equivalent to the number of holes that remain trapped in the SiO₂ and is called the yield which is represented by:

$$\text{Yield} = \int_0^{T_f} \int_{\text{Surface}} n_-(r,t) \text{ velocity } ds dt \quad (6)$$

In this equation, T_f is the total amount of time that is required for the two cylinders to pass each other due to the z component of the electric field.

$$T_f = \frac{L}{\mu_- E \cos^2 \theta} \quad (7)$$

where L is the SiO₂ thickness and E is the magnitude of the electric field.

For the purposes of this model, it is assumed that all of the holes that remain in the SiO₂ will eventually move to the SiO₂-substrate interface and become trapped there. By experimentally measuring the threshold voltage shift, the actual number of holes that became trapped at the interface can be measured with the use of equation 2.

Due to the method in which the code calculates the charge collected, the model tends to underestimate the number of electrons collected at the gate (and thus holes that survive) at early times. In most cases, the majority of the recombinations that do occur happen very rapidly and at times on the order of 10⁻¹⁵ seconds or less. Fortunately, the majority of the charge which is collected is that portion that survives recombination and remains in the cylinders after the two columns have separated in the x direction. Thus the amount of charge collected at early times is generally only a small fraction of the total charge collected. The exceptions to this are those occasions when large amounts of recombination occur throughout the time required for collection of the electrons. Small electric fields and large linear energy depositions are examples where large amounts of recombinations occur.

The Computer Code.

Previously, attempts to solve the Jaffee equation have utilized explicit numerical analysis techniques⁵. The computer method we used to solve the coupled differential equations for this physical system was the Alternating Direction Implicit Method (ADI), also known as the Peachman-Rachford Method⁶. This method is an improvement over the usual explicit method in that it is nearly always stable and convergent. The ADI method involves the solution of a tridiagonal matrix equation which is much simpler and straightforward than the solution to an implicit method system in two dimensions.

For the first half cycle, the calculations proceed along the x axis with the finite elements being implicit in the x direction and explicit in the y direction. This results in the following expression for the electron volume density which is a discrete version of equation 5:

$$\begin{aligned}
& \left[\frac{D\Delta t}{2(\Delta x)^2} - \frac{\mu E \Delta t}{4\Delta x} \right] n_{i-1,j}^{k+1} - \left[\frac{D\Delta t}{(\Delta x)^2} + 1 \right] n_{i,j}^{k+1} + \left[\frac{D\Delta t}{2(\Delta x)^2} + \frac{\mu E \Delta t}{4\Delta x} \right] n_{i+1,j}^{k+1} \\
& = - \left[\frac{D\Delta t}{2(\Delta x)^2} \right] n_{i,j-1}^k + \left[\frac{D\Delta t}{(\Delta x)^2} + \frac{\alpha \Delta t}{2} - 1 \right] n_{i,j}^k - \left[\frac{D\Delta t}{2(\Delta x)^2} \right] n_{i,j+1}^k \quad (8)
\end{aligned}$$

During the second half cycle, the calculations proceed along the y axis with the finite elements being explicit in the x direction and implicit in the y direction. This results in the following expression:

$$\begin{aligned}
& \left[\frac{D\Delta t}{2(\Delta x)^2} \right] n_{i,j-1}^{k+1} - \left[\frac{D\Delta t}{(\Delta x)^2} + 1 \right] n_{i,j}^{k+1} + \left[\frac{D\Delta t}{2(\Delta x)^2} \right] n_{i,j+1}^{k+1} \\
& = - \left[\frac{D\Delta t}{2(\Delta x)^2} - \frac{\mu E \Delta t}{4\Delta x} \right] n_{i-1,j}^k + \left[\frac{D\Delta t}{(\Delta x)^2} + \frac{\alpha \Delta t}{2} - 1 \right] n_{i,j}^k - \left[\frac{D\Delta t}{2(\Delta x)^2} + \frac{\mu E \Delta t}{4\Delta x} \right] n_{i+1,j}^k \quad (9)
\end{aligned}$$

It should be recognized that there is a similar set of equations for the hole density with a reversed sign on the drift term which is solved simultaneously.

The advantage of the ADI method should become clear at this point. Each of the matrix equations that require solution are tridiagonal and may be efficiently solved by LU decomposition⁷. The program begins by calculating the initial cell centered density of electrons and holes for each of the cells. The lower and upper matrix elements are calculated for the initial time element. The main cycling routine consists of the calculation of the known values of equation 8 and the solution of the equation for one row in the x direction. After solving for each of the rows in the x direction, the routine will perform a similar set of calculations based upon equation 9 progressing through each column in the y direction. There being no component of the electric field in the y direction, the problem is symmetric across the x axis and only a half cylinder need actually be calculated.

At the end of each time step the number of electrons that are collected at the gate is calculated. The number collected is related to the portion of the electron cylinder which no longer overlaps the hole cylinder. That portion of the cylinder is indicated in figure 4b. The length of this cylinder element is the product of the electric field along the z axis, the electron mobility in silicon dioxide, and the time element dt. Thus the number of electrons arriving at the gate (and thus the number of holes remaining trapped in the SiO₂) during any time period dt is the total number of electrons in the portion of the cylinder representing the non-recombined electrons which is found by:

$$\text{Yield} = \sum_i \sum_j n(i,j) (\Delta x \Delta y) (\text{element thickness}) \quad (10)$$

The process is considered complete when the recombination rate for any one step is less than .05 percent of the total number of electrons remaining. At this point, the solution assumes that no more recombination will occur and all of

the electrons that currently remain in the column will be collected at the gate. The ratio of the number of holes that survive to the total number of electron-hole pairs created is called the fractional yield.

The values used in this analysis for the various constants are given below:⁸

electron mobility	$\mu_- = 40 \text{ cm}^2/\text{V-s}$
hole mobility	$\mu_+ = 10^{-5} \text{ cm}^2/\text{V-s}$
recombination coefficient	$\alpha = 1.88 \times 10^{-5} \text{ cm}^3/\text{s}$
diffusion coefficient	$D_- = 0.261 \text{ cm}^2/\text{s}$
diffusion coefficient	$D_+ = 6.5 \times 10^{-8} \text{ cm}^2/\text{s}$
column width	$b = 3.5 \text{ nm}$

The thickness of the SiO₂ layer, electric field strength, angle of incidence and linear density of electron-hole pairs are considered to be variables in the program and are required input. As the program cycles, the electron and hole volume densities along the x axis are plotted for each cycle on the screen. While this plotting does slow the program, it is a useful tool in understanding the physics of what is happening inside the cylinders. The final output of the program is a recapitulation of the initial parameters, the fractional yield and the change in threshold voltage per particle.

Results and Analysis.

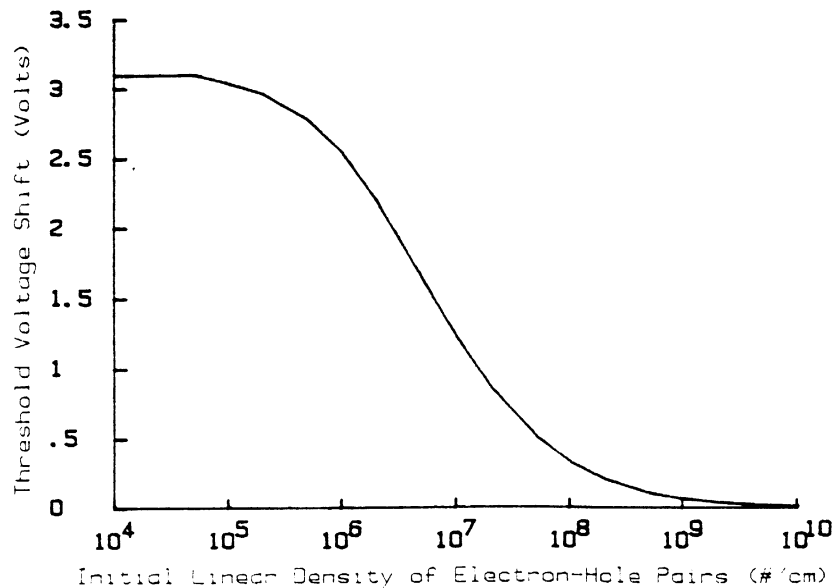


Figure 5. Threshold Voltage Shift vs Initial Linear Pair Density.

Figure 5 is a plot of the predicted threshold voltage shift vs the initial electron-hole linear density (and thus the initial linear energy density). The plot is made for particles impacting at an angle of incidence of 45 degrees on a device with a 350 nm oxide layer under a 5 volt gate voltage ($E = 1.4 \text{ MV/cm}$). A dose of 1 krad is assumed for all cases. Note that while the energy

deposited is constant, the damage done varies considerably with the initial linear energy density. This implies that while the high energy, extremely heavy ions in cosmic rays (for example iron) will deposit large amounts of energy in the device, the damage due to ionization effects from these ions will be small. This is because their high linear energy density leads to large amounts of recombination.

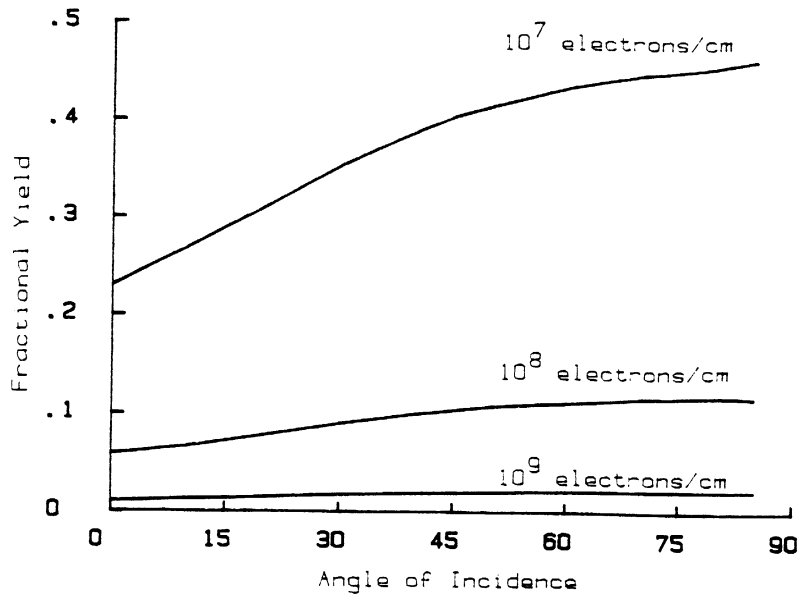


Figure 6. Fractional Yield vs The Angle of Incidence For Various Initial Energy Densities.

Figure 6 is a plot of the fractional yield vs the angle of incidence for various initial electron-hole linear densities. The plot is made for a device with a 350 nm oxide layer under a 5 volt gate voltage ($E = 1.4$ MV/cm). This graph helps to explain the observed dependence of the threshold voltage shift with angle for protons which was observed by Tallon⁹. He also observed that for low proton energies (which have a high linear energy density) the variation in threshold voltage shift with angle between 45 degrees and 80 degrees became almost nonexistent, while for high proton energies (low linear density) the variation was clear. The computer model also predicts such behavior as a result of the high initial density of electron-hole pairs. At high densities, the initial recombination rate is so high that the rate of separation becomes meaningless. This model demonstrates that the effect is not caused by a buildup of charge on the SiO₂-substrate interface which reduces the effective electric field as Tallon believed but is a consequence of the high linear energy deposition of the particles.

Preliminary Experimental Verification.

Several n-channel devices were irradiated with protons at the USMA Particle Accelerator Laboratory. The gate size of each device was 3 μ m by 8 μ m with

an oxide thickness of approximately 960 nm. The devices were bombarded with either a diffuse 340 keV or 500 keV proton beam. The proton energies are known with less than 1 percent uncertainty based upon the (p, γ) resonances of boron (163.1 keV) and fluorine (340.6 keV). Proton flux was measured before each irradiation by passing the beam through collimators of known area and collecting the charge deposited with a current integrator. Each device was irradiated with a dose of 500 krads. This was done by rotating the device into the beam for a calculated amount of time based upon the desired dose, proton flux and device size, and then rotating it out of the beam. The threshold voltage for each device was measured before and after irradiation by graphically plotting the I-V curve for the device. The gate voltage (V_{GS}) was maintained at 5 volts during irradiation and until the I-V curve could be measured.

The linear energy density is found from the stopping power equation for protons¹⁰:

$$\frac{\partial E}{\partial x} = \frac{4.978 S_{high} S_{low}}{S_{high} + S_{low}} \text{ keV}/\mu\text{m} \quad (11)$$

$$S_{low} = 4.7 E^{0.45}$$

$$S_{high} = (3329/E) \ln[1 + (550/E) + (0.01321 E)]$$

Where E is then energy of the bombarding proton in keV. The energy required to create one electron-hole pair is 18 eV^{11} . Thus the stopping power is directly related to the linear density of electron or holes.

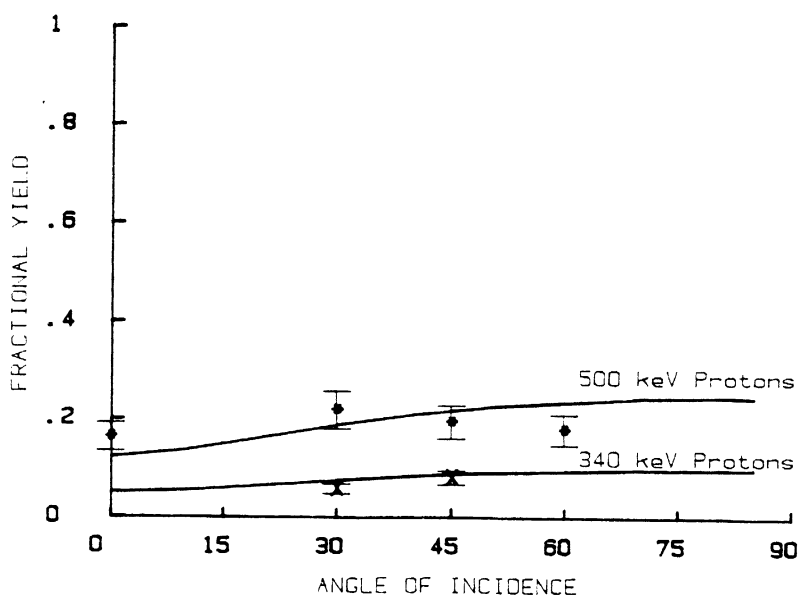


Figure 7. Comparison of Computer Predictions and Test Samples For Proton Energies of 340 keV and 500 keV

The results of the test devices are shown in figure 7. Because of the uncertainties associated with the magnitude of the dose, the uncertainty in the fractional yield is quite high. However, the results do indicate that further and more accurate testing is warranted to verify the predictions made above.

Conclusion.

One of the most interesting results of this work is that while radiation damage is commonly measured in rads (energy deposited), our results show that the amount of damage produced by one rad of radiation can vary greatly (as measured by the threshold voltage shift). The damage done to a device is a complex function of many of the physical parameters, most notably the angle of incidence and the magnitude of the applied electric field, as well as the rate of linear energy deposition (stopping power) of the incident particle.

A logical extension of this work is that the damage done by electrons (thus x rays and gamma rays as well) should be considerably greater than the damage done by an ion which deposits the same amount of energy. The high recombination rate observed in this study is the result of the high electron-hole density along the path of the ion. Since electrons lose their initial direction and tend to have a much more diffuse energy deposition^{1,2}, the recombination rate will be much less and the damage will be greater for the same amount of energy deposited.

There are some improvements yet to be made on the computer code. Charge would be better modeled as being stripped off in an elliptically shaped cylinder with a thickness based upon the total electric field strength rather than only the z component. More precise measurements on electronic devices must be made to further confirm or disprove the details of the model. The validity of the assumption that all of the holes left in the SiO₂ layer will travel to the SiO₂-substrate interface is uncertain. Prompt measurements of the threshold voltage shifts after irradiation and extending over time should enable measurement of the amount of recombination that occurs as the holes move to the interface.

Acknowledgments

The authors would like to thank Dr. T. R. Oldham and Dr. J. M. McGarrity, without whose assistance this study would not have been possible. A special thanks is due Mr. R. Ronson who machined the device holders and accelerator parts required.

References

1. M. Eisenbud, ENVIRONMENTAL RADIOACTIVITY (Academic Press, New York, 1973), pp. 192-6.
2. A. Bar-Lev, SEMICONDUCTORS AND ELECTRONIC DEVICES, (Prentice/Hall, London, 1979), p. 193-9.
3. G. Jaffee, Annalen der Physik, 42, (1913), p. 303.
4. Solutions to the problem are not sensitive to the shape of initial distribution assumed and vary by less than 10% as long as the peak linear density is constant.

5. T. R. Oldham, CHARGE GENERATION AND RECOMBINATION IN SILICON DIOXIDE FROM HEAVY CHARGED PARTICLES, (Harry Diamond Laboratories, HDL-TR-1985, Adelphi, Md)
6. The program is written in QUICK BASIC for an IBM PC or compatible. A copy of the program may be obtained by sending a diskette to the authors.
7. L. W. Johnson, R. D. Riess, NUMERICAL ANALYSIS, (Addison-Wesley, Reading, Ma., 1982), p. 40-1.
8. T. R. Oldham, op. cit.
9. R. W. Tallon, W. T. Kemp, M. R. Ackerman, M. H. Owen, and A. H. Hoffland, RADIATION DAMAGE IN MOS TRANSISTORS AS A FUNCTION OF THE ANGLE BETWEEN AN APPLIED ELECTRIC FIELD AND VARIOUS INCIDENT RADIATIONS (PROTONS, ELECTRONS, AND CO-60 GAMMA RAYS), IEEE Transactions on Nuclear Science, Volume NS-34, Number 6, December 1987.
10. J. F. Ziegler, THE STOPPING POWER AND RANGES OF IONS IN MATTER 3, (Pergamon Press, New York, 1977).
11. V. A. J. van Lint, T. M. Flanagan, R. E. Leadon, J. A. Naber, and V. C. Rogers, MECHANISM OF RADIATION EFFECTS IN ELECTRONIC MATERIALS, Vol 1, (Wiley and Sons, New York, 1980), p. 222.
12. N. Tsoulfanidis, MEASUREMENT AND DETECTION OF RADIATION, (McGraw-Hill, New York, 1983), p. 118-30.